*Friction* **3**(1): 72–81 (2015)
DOI 10.1007/s40544-015-0076-4
ISSN 2223-7690
CN 10-1237/TH

RESEARCH ARTICLE

# *In situ* reduction and functionalization of graphene oxide to improve the tribological behavior of a phenol formaldehyde composite coating

**Mingming YANG[1,2], Zhaozhu ZHANG[1,*], Xiaotao ZHU[1], Xuehu MEN[1,*], Guina REN[1,2]**

[1] *State Key Laboratory of Solid Lubrication, Lanzhou Institute of Chemical Physics, Chinese Academy of Sciences, Tianshui Road 18th, Lanzhou 730000, China*

[2] *University of Chinese Academy of Sciences, Beijing 100039, China*

*Received: 17 October 2014 / Revised: 20 January 2015 / Accepted: 01 March 2015*



**Abstract:** The development of a phenol formaldehyde/graphene (PF–graphene) composite coating with high performance is desirable but remains a challenge, because of the ultrahigh surface area and surface inertia of the graphene. Herein, we synthesized PF–graphene composites by the *in situ* polymerization of phenol and formaldehyde with the addition of graphene oxide, resulting in improved compatibility between the graphene and phenolic resin (PF) matrix and endowing the phenolic resin with good thermal stability and excellent tribological properties. Fourier-transform infrared (FTIR) spectra and X-ray diffraction (XRD) patterns demonstrated that the graphene oxide was reduced during the *in-situ* polymerization. The PF–graphene composites were sprayed onto steel blocks to form composite coatings. The effects of an applied load and of the sliding speed on the tribological properties of the PF–graphene composite coating were evaluated using a block-on-ring wear tester; in addition, the worn surface and the transfer film formed on the surface of the counterpart ring were studied by scanning electron microscopy (SEM). The results show that the PF–graphene composite coating exhibited enhanced tribological properties under all tested conditions.

**Keywords:** wear; friction; graphene; phenolic resin

## 1 Introduction

Phenolic resins (PF), notwithstanding their century-long history, continue to attract a great deal of research interest. Because of their thermal stability, high char yield, structural integrity, and solvent resistance, they are widely used as coatings, thermal insulation, aeronautic applications, electro-optical devices and composite materials [1, 2]. Extensive research has been conducted to improve the friction and wear properties of phenolic resin and its composites via the incorporation nanoparticles into the phenolic resin matrix [3, 4]. However, numerous groups have reported that nanoparticles are difficult to disperse into the polymer matrix by mechanical dispersive mixing because of the agglomeration of nanoparticles and the high viscosity of polymer [5].

Graphene has inspired enormous research interests in the fabrication of functional polymer composites because of its high aspect ratio and unique electrical, mechanical and thermal properties [6–9]. Due to this excellent properties, the graphene reinforced polymer composites have been widely applied as coatings, liners, ablative materials, and in aerospace applications. Two primary popular approaches have thus far been devised for the preparation of graphene. One approach is to thermally exfoliate graphene oxide (GO) at high temperatures in a furnace, during which thermal reduction occurs; the other approach is to ultrasonically exfoliate graphene oxide to graphene in solvents or

* Corresponding author: Zhaozhu ZHANG; Xuehu MEN.
E-mail: zzzhang@licp.cas.cn (Z. Z); xhmen@licp.cas.cn (X. H. M)

polymer/monomer solutions and then chemically reduce the GO [10–14]. To improve the dispersion of graphene sheets in polymer matrices, chemical functionalization of the graphene sheets is required to enhance their compatibility with polymers [15, 16]. GO has been reported to be reduced during *in-situ* polymerization [17, 18]. Xu et al. reported that nano-scale graphene oxide can be well dispersed in the matrix of PF by *in situ* polymerization and that the thermal stability and dynamic mechanical properties of the GO/PF composites were significantly improved [19]. Xu et al. reported that a graphene-reinforced Nylon-6 composite with a graphene loading of 0.1 wt%, which they prepared by an *in situ* polymerization approach, exhibited excellent tensile strength and a high Young's modulus [20]. However, the tribological properties of graphene oxide/PF composites prepared by *in-situ* chemical reduction and functionalization have rarely been reported.

To endow PF with excellent tribological properties, we used a facile approach to reduce and functionalize GO during *in-situ* polymerization of phenol and formaldehyde in the presence of GO sheets. Subsequent characterization confirmed that GO was reduced and functionalized during the *in-situ* polymerization, which improved the compatibility between graphene and the PF matrix. The results showed that the PF–graphene composite coating exhibited optimal tribological properties under all tested conditions.

## 2 Experimental details

### 2.1 Materials

Phenol (99%) and formaldehyde solution (37%) were purchased from Xi Long Chemical Company. Graphite powder was purchased from the National Medicine Company of Shanghai, China. Polyfluo 150 wax (PFW) as a powder with a particle diameter of approximately 3–4 μm was provided by Micro-Powders Inc. An AISI 1045 block (12.7 mm × 12.7 mm × 19 mm) was used as the substrate of the phenolic composite coating. An AISI-C-52100 steel ring with a diameter of 49.24 mm and a thickness of 12 mm (hardness Hv850) was rotated against the phenolic composite coatings under dry friction conditions. The chemical compositions of the 1045 steel and the AISI-C-52100 bearing steel are shown in Table 1.

### 2.2 Synthesis of PF–graphene composites

Graphene oxide was prepared from natural graphite using a modified Hummers' method described in Refs. [21–23]. The PF–graphene was prepared according to previously reported procedures [15]. PF–graphene composites were prepared using a formaldehyde/phenol (F/P) molar ratio of 1.32 in the presence of sodium hydroxide. Typically, phenol, formaldehyde, and graphene oxide were added into a three-neck flask. After the pH was adjusted to 9.0, the mixture was ultrasonicated at 70 ℃ for 2 h, and subsequently heated to 85 ℃ for 2.5 h in an oil bath. The reaction was stopped when the viscosity of the mixture increased dramatically. At the end of the reaction, water was removed under vacuum at 70 ℃, and a black product was obtained. The obtained black product was designated as PF–graphene composite. Four kinds of PF–graphene composites with different graphene oxide contents (0.1, 0.2, 0.3, and 0.4 wt%) were prepared.

### 2.3 Preparation of composite coating

The SISI 1045 block (12.7 mm × 1.2.7 mm × 19 mm) was polished with 300 grade water proof abrasive paper and then cleaned with acetone in an ultrasonic bath for 10 min. The PFW and PF–graphene were dispersed in ethanol with ultrasonic stirring for 1 h. The amount of the solid lubricant PFW used was 20 wt% relative to the amount of phenolic binder. The coatings on blocks were prepared by spraying the coating pre-cursors using 0.2 MPa nitrogen gas and then cured at 85 ℃, 120 ℃, and 180 ℃ for 2 h, respectively.

**Table 1** The chemical composition of the AISI-C-52100 bearing steel and steel 45 (in wt.%).

| | C | Si | Mn | P | S | Cr | Ni | Cu | Fe |
|---|---|---|---|---|---|---|---|---|---|
| Steel 45 | 0.42–0.5 | 0.17–0.37 | 0.50–0.80 | 0.035 | 0.035 | 0.25 | 0.25 | 0.25 | Balance |
| Bear steel | 0.98–1.1 | 0.15–0.35 | 0.25–0.45 | | | 1.3–1.6 | | | Balance |

### 2.4 Characterization

Fourier transform infrared (FTIR) spectra were collected on a Bruker IFS66 V/S spectrometer. Thermogravimetric analysis (TGA) was carried out using a thermogravimetric analyzer (STA 449F3) with the samples under a nitrogen atmosphere. X-ray powder diffraction (XRD) patterns were obtained using a Rigaku D/Max X-ray diffractometer. The morphology of the worn surface was observed by scanning electron microscopy (SEM, JEOLJSM-5600LV). FEI Tecnai F30 transmission electron microscopy (TEM, FEI Tecnai F30) was used to investigate the microstructure and morphology of the graphene and PF–graphene.

An MHK-500 ring-on-block wear tester (manufactured by the Jinan Testing Machine Factory, China) was used to evaluate the friction and wear behaviors of the PF–graphene composite coating (see Fig. 1). A steel ring was rotated against the PF–graphene composite coatings at speeds of 2.24–3.68 m/s and loads of 320–620 N under different sliding conditions. Before each test, the steel ring and the coating were abraded with 900 grade water proof abrasive paper. Then they were cleaned with acetone and dried. The sliding distance was calculated from the product of the sliding speed and the sliding time. The wear life of the PF–graphene composite coatings was calculated by dividing the sliding distance by the corresponding wear depth in micrometers. Wear depth was measured using a micrometer (± 0.001 mm). Thus the friction and wear tests were conducted at 20–25 °C and at a relative humidity of 30%–50%, and the data presented in the current work represent the averages of three replicate measurements.

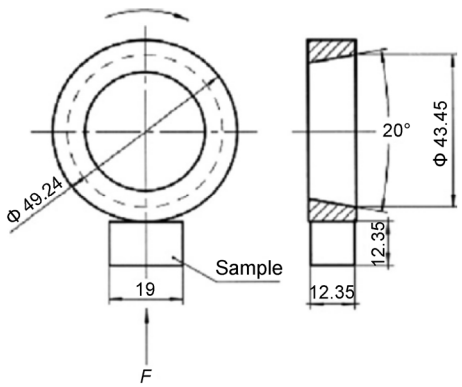


**Fig. 1** Contact schematic for the frictional couple.

## 3 Results and discussion

### 3.1 Characterization of the PF–graphene composite

Figure 2(a) shows the FTIR spectra of GO, PF–graphene, and PF. In the spectrum of GO, the characteristic absorption peaks appear at 1,698 $cm^{-1}$ and 1,620 $cm^{-1}$, and these peaks are attributed to the C=O and C=C stretching vibrations, respectively. In the spectrum of PF, the peaks at 2,917 $cm^{-1}$, 2,849 $cm^{-1}$ and 1,474 $cm^{-1}$ correspond to the –CH stretching and bending vibrations. The C=C stretching vibration of the phenolic ring appears at 1,638 $cm^{-1}$. By comparison with the spectra of PF and GO, the appearance of absorption peaks in the spectrum of PF–graphene at 2,911 $cm^{-1}$, 2,836 $cm^{-1}$ (–$CH_2$ stretching), 1,609 $cm^{-1}$ (C=C stretching), 1,476 $cm^{-1}$ (–$CH_2$ bending), and 1,051 $cm^{-1}$ (methylol stretching), indicated the graphene oxide was reduced and functionalized by PF chains [9, 24]. Furthermore, the weakened peak at 1,358 $m^{-1}$, which is assigned to the O–H deformation vibration of PF and the new C–O stretching vibration at 1,142 $cm^{-1}$ imply that the nucleophilic substitution reaction occurred between the PhO-groups of the PF prepolymer and the oxygen containing groups of GO [9]. Phenolate anions are known to act as a nucleophil to functionalize GO [25].

The XRD spectra of graphene oxide, graphene, and PF–graphene are shown in Fig. 2(b). Because of the absence of functional groups containing oxygen after the reduction of GO, the intra-gallery spacing decreased from 9.358 Å (10.5°) in graphene oxide to 4 Å (24.4°). This decrease in interlayer spacing indicated that aggregation persisted to some extent. Such aggregation presumably arises from the strong van der Waals interactions between the sheets of the reduced graphene. Compared with the graphene, however, the interlayer spacing of PF–graphene was enlarged from 4 Å (24.4°) in the case of reduced graphene to 5.36 Å (18.36°) after functionalization of graphene oxide via *in situ* chemical reduction. The XRD results demonstrated that the graphene oxide was reduced via the *in situ* polymerization process, consistent with the FTIR results [15].

The dispersion stability of pristine graphene and PF–graphene prepared in ethanol was evaluated by visual observation at different standing times after sonication (Fig. 3). Immediately after sonication

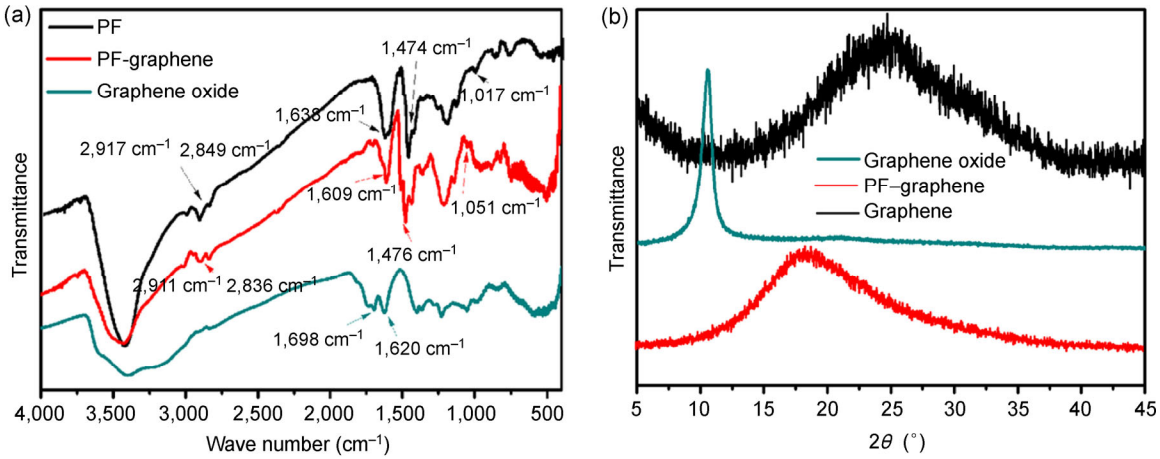


**Fig. 2** FTIR (a) and XRD (b) analysis for the PF, PF–graphene, and graphene oxide.

(Fig. 3(a)), both the graphene and the PF–graphene sheet were black, and the two solutions were uniform. With increasing sonication time, the pristine graphene sheet solution contained some suspended sheet aggregates, and the graphene finally completely settled to the bottom of the bottle after 3 days (see bottle A in Figs. 3(b) and 3(c)). However, the PF–graphene/ethanol solutions were always stable (see bottle B in Fig. 3). These phenomena indicate that *in-situ* reduction and functionalization of graphene oxide during the polymerization of the phenol and formaldehyde can considerably improve the solubility of the graphene. The presence of the phenolic resin layer on the graphene was confirmed by TEM (Figs. 3(d) and 3(e)) images. We observed that in comparison to the clear image of the graphene surface (Fig. 3(d)), the PF–graphene image (Fig. 3(e)) shows a fine coating that uniformly cover the graphene surface uniformly. Therefore, we reasonably concluded that the phenolic chain was grafted onto the graphene surface.

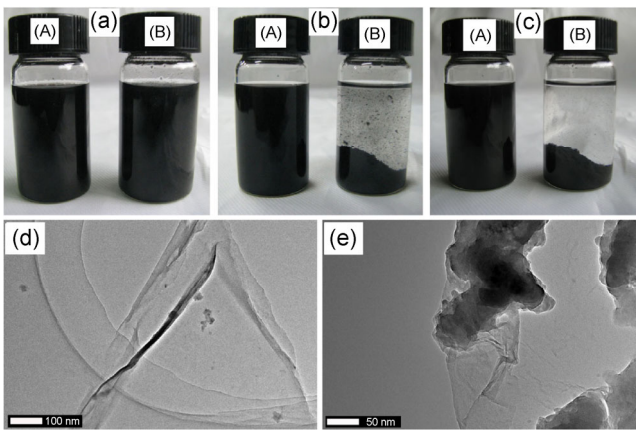


**Fig. 3** Stability of the graphene and PF–graphene/ethanol dispersions observed at different time: (a) immediately; (b) t~2h; (c) t~3d. ((A): PF–graphene; (B): pristine graphene) and TEM images (d) pristine graphene; (e) PF–graphene.

Thermal stability was assessed by TGA under a nitrogen atmosphere, and the resulting thermograms are shown in Fig. 4. The two phenolic resins both exhibit a small mass loss (1.3%) at approximately 150 ℃ due to the removal of adsorbed water. However, the residual weight of the PF–graphene was greater than that of PF in the temperature range between 150 and 595 ℃. Table 2 shows the degradation temperatures ($T_d$) for PF, and PF–graphene. Compared with the $T_d$ of PF, the $T_d$ for PF–graphene was higher because of the addition of graphene. The result demonstrated that the thermal stability of the phenolic was improved by the *in-situ* chemical reduction and functionalization of graphene oxide.

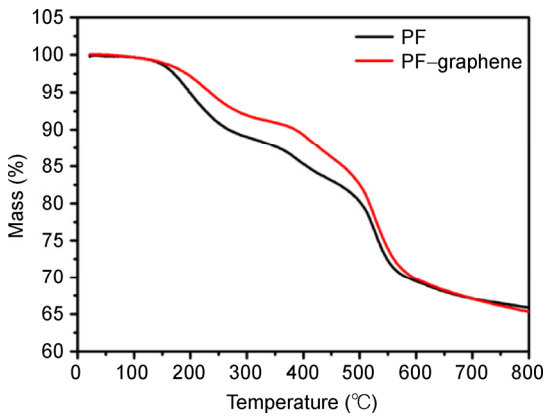


**Fig. 4** TGA analysis for PF and PF–graphene.

**Table 2** Thermal property of two phenolic resins.

| weight loss (wt%) | Temperature for PF | Temperature for PF–graphene |
|---|---|---|
| 5% | 198 | 234 |
| 10% | 268 | 384 |
| 20% | 502 | 517 |
| 30% | 583 | 593 |

### 3.2 The effect of graphene oxide loading on the tribological properties of the composite coating

Figure 5 shows the effect of graphene oxide content on the wear life and friction coefficient of PF and PF–graphene composite coatings under an applied load of 320 N, a sliding speed 2.24 m/s, and dry sliding conditions. The data refer to the mean values measured in the steady state range of the wear process. The results showed a monotonic increase in wear life with increasing graphene oxide content when the graphene oxide content was less than 0.3 wt%. However, the friction coefficient initially decreased and then increased with increasing graphene oxide content. Because of the strong van der Waals interactions between the reduced graphene sheets, they are prone to agglomerate when a large mass fraction of the graphene is added to phenolic resin. This agglomeration may lead to drawing out of the graphene from the matrix resin during the test. Thus, abrasion occurred and the friction coefficient increased when the filler content was excessive [26]. This result indicated that appropriate filler content could improve the tribological behavior of the PF–graphene composite coating. The results showed that the best friction-reduction was achieved at a concentration of 0.3 wt%. The friction reduction and anti-wear ability of the 0.3% graphene oxide loading can be explained by good dispersion. Thus, 0.3 wt% was chosen as the optimal graphene oxide content of the phenolic composite coating. Compared with the PF composite coating (289.5 MPa, 3.61 GPa), graphene had little effect on the hardness and Young's modulus of the PF–graphene composite coating (286 MPa and 3.94 GPa).

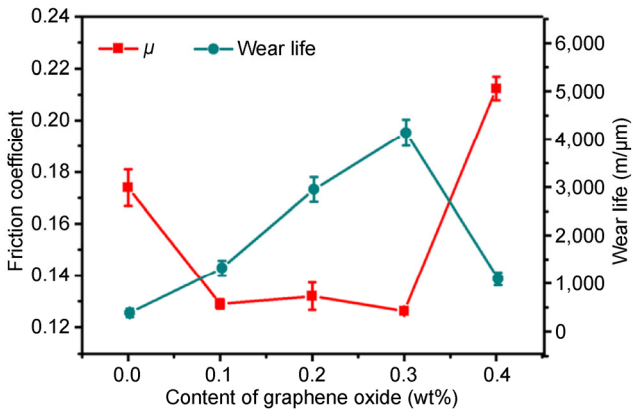


**Fig. 5** The effect of graphene oxide content on the friction and wear performance of the composite coatings (sliding speed: 2.24 m/s, applied load: 320 N, test time: 60 min).

Figure 6 shows SEM images of the two phenolic composite coatings surfaces and sections. In the case of PF–graphene composite coating, the substrate was well bonded with the PF–graphene coating matrix, and gaps were not apparent at the filler/matrix interface (see Fig. 6(d)). Moreover, no cavities were evident on the surface of the PF–graphene composite coating surface (see Fig. 6(b)). This lack of cavities is attributed to excellent adhesion between the functionalized graphene and the phenolic matrix. In contrast, numerous cavities were apparent in the surface and section of the pure phenolic composite coating (see Figs. 6(a) and 6(c)), which might have been caused by solvent evaporation.

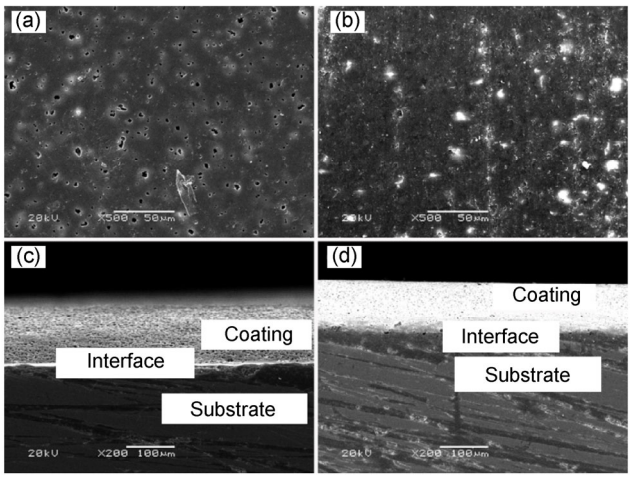


**Fig. 6** (a) and (b) is the SEM image of the surface morphology for PF composite coating and PF–graphene composite coating, respectively; (c) and (d) is the corresponding cross section image for PF composite coating and PF–graphene composite coating, respectively.

### 3.3 The effect of applied load on the tribological properties of the composite coatings

The variations of the friction coefficient and the wear life of the two phenolic composite coatings under various applied loads, where the tests were conducted under dry conditions at a sliding speed of 2.24 m/s, are shown in Fig. 7. Evidently, the friction coefficient (Fig. 7(a)) and the wear life (Fig. 7(b)) of the two phenolic composite coatings both decreased with increasing load. A comparison of the tribological behaviors of the pure PF composite coating, revealed that the coating of phenolic resin composite containing graphene reduced *in situ* exhibited excellent tribological properties. Because polymers are a visco-elastic materials the variation of the friction coefficient under an applied load follows the equation $\mu = KN^{n-1}$ where $\mu$ is the friction coefficient, $N$ is the load, $K$ and $n$ are constant, $2/3<n<1$ [27]. According to this equation, the friction coefficient decreases with increasing load. Experimentally, the graphene slid easily and prevented catastrophic failure of the brittle phenolic matrix by detouring fatigue cracks [28]. Therefore, the PF–graphene composite coating exhibited a lower friction coefficient and greater wear life than the composite coating without graphene when tested at a sliding speed of 2.24 m/s and a load of 320–620 N. The weak van der Waals interaction between the lamellaes of the graphene nanosheets provides low resistance to shear under the rolling contact stress, resulting in reduced in friction. Furthermore, the continuous supply of these nanosheets on the contact surfaces, because of their stable dispersion in the phenolic matrix, avoids direct contact between samples and the counterpart ring and improves the anti-wear properties of the PF–graphene composite coating [29].

Figure 8 presents SEM micrographs of the worn surface of the two phenolic composite coatings. As evident in the figure, the worn surface of the pure PF composite coatings exhibit severe scuffing with numerous deep and narrow grooves and extensive peeling of the phenolic resin from the matrix (Fig. 8(a)). However, in case of the PF–graphene composite coating, the wear surface was relatively smooth, and exhibited only fine scratches (Fig. 8(b)). The tribological behavior of the phenolic resin composite coatings is strongly influenced by their ability to form transfer films on the counterface. After transfer films are formed, subsequent interaction occurs between the polymer coating and the transfer films of similar composition instead of between the polymer coating and the steel counterface [30]. To further study the friction and wear mechanism of the coating, we investigated the micrographs of the counterpart surface. As evident in Fig. 8(c), the transfer film of the PF coating appeared to be rough and discontinuous. In contrast, the transfer film of the PF–graphene composite coating (Fig. 8(d)) appeared to be much smoother than that of the PF composite coating.

### 3.4 The effect of sliding speed on the tribological properties of the composite coatings

The friction coefficient and wear life of the two phenolic composite coatings at different sliding speeds under

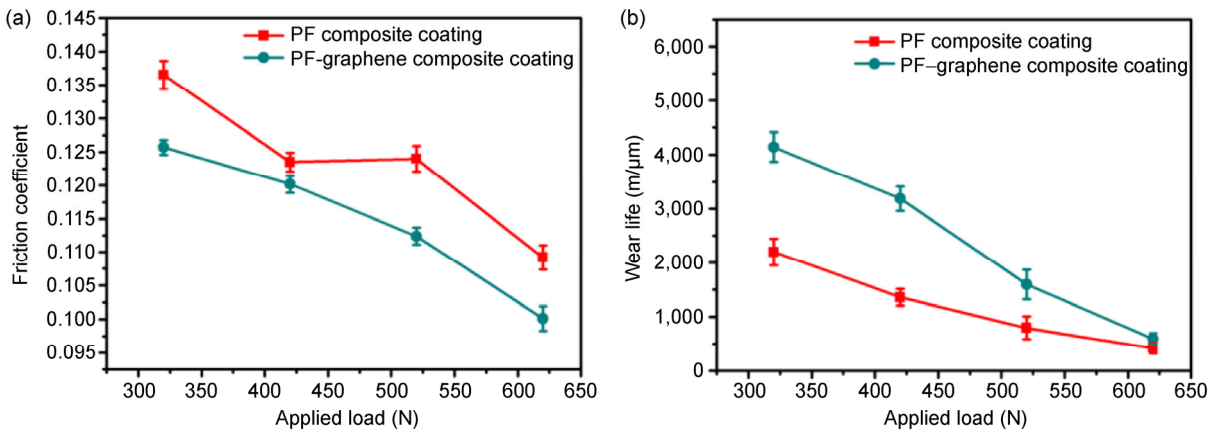


**Fig. 7** The effect of applied load on the friction and wear behaviors of the two composite coating (sliding speed: 2.24 m/s, test time: 60 min).

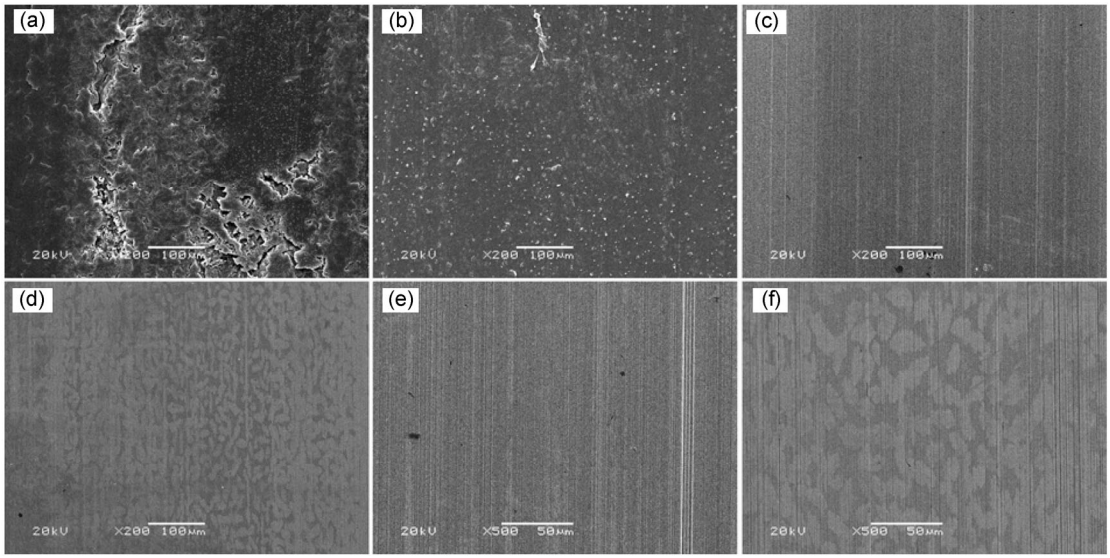


**Fig. 8** SEM pictures of the worn surface (a) PF composite coating; (b) PF-graphene composite coating; (c) the transfer film of (a); (d) the transfer film of (b); (e) and (f) are magnified image of (c) and (d). The applied load, sliding speed, and test time is 320 N, 2.24 m/s, and 60 min, respectively.

an applied load of 320 N are shown in Fig. 9. As evident in the figure, the two composite coatings exhibited greater friction coefficients at low sliding speeds. As the sliding speed was increased further, however, the friction coefficient decreased which we attributed to surface softening arising from frictional heating. Moreover, the wear life of the two composite coatings decreased with increasing sliding speed. Accordingly, the PF–graphene composite coating exhibited the best anti-wear behavior among the investigated coatings. The graphene in the composite coating will slowly release onto the metal surface during the wear and friction tests, and more easily slide between the two mating surfaces, resulting in a decrease in the friction coefficient. In addition, the graphene on the surface serves as a spacer, that prevents rough contact between the two mating surfaces, thereby enhancing the wear life considerably.

The SEM morphologies of the worn surface of the PF–graphene composite coating under an applied load of 320 N at different sliding speeds are shown in Fig. 10. The PF–graphene composite coating was characterized by mild scuffing and little matrix peeling (Fig. 10(a)). This observation is consistent with the

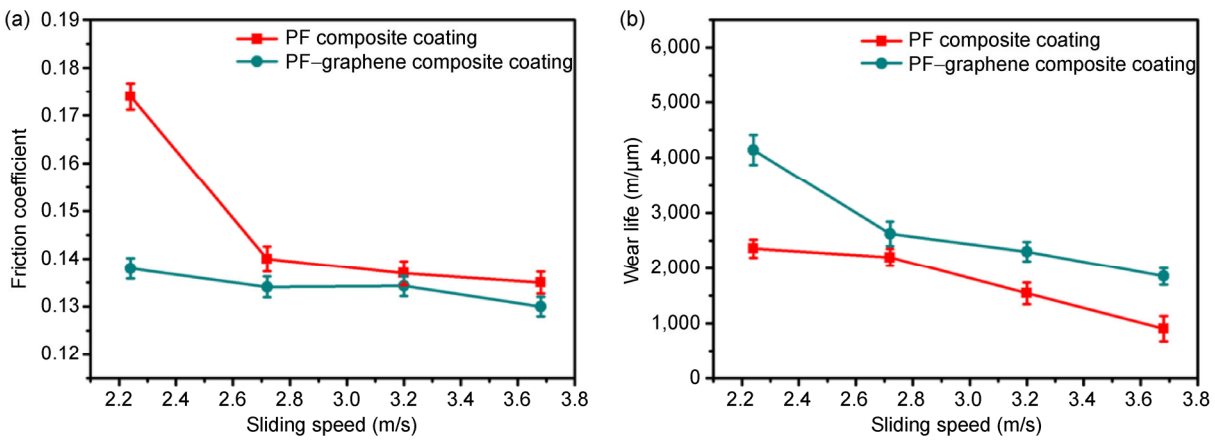


**Fig. 9** The effects of sliding speed on the friction and wear behavior of the two composite coatings. The applied load and test time is fixed to 320 N and 60 min, respectively.

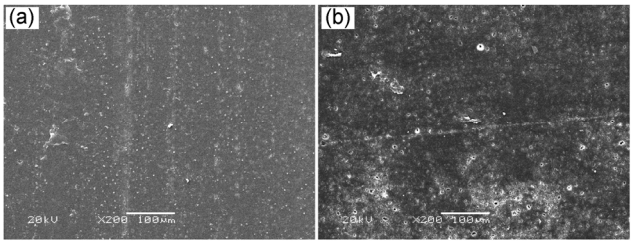


**Fig. 10** SEM photographs of the worn surface of the PF–graphene composite coating under the sliding speed of (a) 2.72 m/s and (b) 3.2 m/s. The applied load and test time is fixed to 320 N and 60 min.

greater wear life of the PF–graphene composite coating compared to that of the PF composite coating. In addition, the worn surface was still smooth and some debris appeared under high sliding speeds (Fig. 10(b)). This observation is attributed to the thermal conductivity of the PF–graphene coating. The enhanced thermal conductivity of a polymer composite is well known to facilitate heat transport and increase the composite thermal stability through the incorporation of highly thermally conductive graphene [31].

## 4 Conclusion

We used a facile approach to reduce and functionalize graphene oxide during the polymerization of phenol and formaldehyde, which resulted in increased interfacial interaction between the graphene and the phenolic resin. We demonstrated that this approach is an effective method of further enhancing the nano-effect of the graphene on the tribological performance of a composite coating. In addition, the applied load and sliding speed were observed to strongly affect the phenolic composite coating. Increases in the applied load and sliding speed, decreased the wear life of the phenolic composite coating. Because, under a high applied load or high sliding speed, friction heat was accumulated and could not be efficiently dissipated, which resulted in depredation of the phenolic composite.

## Acknowledgements

The authors acknowledge the financial support of the National Natural Science Foundation of China (Grant Nos. 51375472 and 51305429).



## References

[1] Wu H H, Chu P P. Degradation kinetics of functionalized novolac resin. *Polym Degrad Stabil* **95**:1849−1855 (2010)

[2] Liu C Q, Li K Z, Li H J, Zhang S Y, Zhang Y L. The effect of zirconium incorporation on the thermal stability and carbonized product of phenol formaldehyde resin. *Polym Degrad Stabil* **102**: 180−185 (2014)

[3] Liu N, Wang J Z, Chen B B, Han G F, Yan F Y. Enhancement on interlaminar shear strength and tribological properties in water of ultra high molecular weight polyethylene/glass fabric/phenolic laminate composite by surface modification of fillers. *Mater Design* **55**: 805−811 (2014)

[4] Song H J, Zhang Z Z, Luo Z Z. Effects of solid lubricants on friction and wear behaviors of the phenolic coating under different friction conditions. *Surf Coat Tech* **201**: 2760−2767 (2006)

[5] Wang H Y, Lu R G, Huang T, Ma Y N, Cong P H, Li T S. Effect of grafted polytetrafluoroethylene nanoparticles on the mechanical and tribological performances of phenol resin. *Mater Sci Eng A* **528**: 6878−6886 (2011)

[6] Layek R K, Nandi A K. A review on synthesis and properties of polymer functionalized graphene. *Polymer* **54**: 5087−5103 (2013)

[7] Ma H L, Zhang H B, Hu Q H, Li W J, Jiang Z G, Yu Z Z, Dasari A. Functionalization and reduction of graphene oxide with p-phenylene diamine for electrically conductive and thermally stable polystyrene composites. *ACS Appl Mater Interfaces* **4**: 1948−1953 (2012)

[8] Yu A P, Ramesh P, Itkis M E, Bekyarova E, Haddon R C. Graphite nanoplatelet–epoxy composite thermal interface materials. *J Phys Chem C* **111**: 7565−7569 (2007)

[9] Layek R K, Nandi A K. A review on synthesis and properties of polymer functionalized Graphene. *Polymer* **54**: 5087−5103 (2013)

[10] Dikin D A, Stankovich S, Zimney E J, Piner R D, Dommett G H B, Evmenenko G, Nguyen S T, Ruoff R S. Preparation and characterization of grapheme oxide paper. *Nature* **448**: 457−460 (2007)

[11] Li W J, Tang X Z, Zhang H B, Jiang Z G, Yu Z Z, Du X S, Mai Y W. Simultaneous surface functionalization and reduction of graphene oxide with octadecylamine for

electrically conductive polystyrene nanocomposites. *Carbon* **49**: 4724−4730 (2011)

[12] Si Y C, Samulski E T. Exfoliated graphene separated by platinum nanoparticles. *Chem Mater* **20**: 6792−6797 (2008)

[13] Tang Z H, Zhuang J, Wang X. Exfoliation of graphene from graphite and their self-assembly at the oil−water interface. *Langmuir* **26**(11): 9045−9049 (2010).

[14] Sun Z Z, James D K, Tour J M. Graphene chemistry: Synthesis and manipulation. *J Phys Chem Lett* **2**: 2424−2432 (2011)

[15] Yuan F Y, Zhang H B, Li X F, Ma H L, Li X Z, Yu Z Z. *In situ* chemical reduction and functionalization of graphene oxide for electrically conductive phenol formaldehyde composites. *Carbon* **68**: 653−661 (2014).

[16] Liu L, Yang J, Meng Q H. The preparation and characterization graphene-cross-linked phenol-formaldehyde hybrid carbon xerogels. *J Sol-Gel Sci Technol* **67**: 304−311 (2013)

[17] Mylvaganam. K, Zhang L C. *In situ* polymerization on graphene surfaces. *J Phys Chem C* **117**:2817−2823 (2013)

[18] Das S, Wajid A S, Shelburne J L, Liao Y C, Green M J. Localized *in situ* polymerization on graphene surfaces for stabilized graphene dispersions. *ACS Appl Mater Interfaces* **3**: 1844−1851 (2011)

[19] Xu W H, Wei C, Lv J, Liu H G, Huang X H, Liu T X. Preparation, characterization, and properties of *in situ* formed graphene oxide/phenol formaldehyde nanocomposites. *J Nanomaterials* 2013: 319840 (2013)

[20] Xu Z, Gao C. *In situ* polymerization approach to graphene-reinforced Nylon-6 composites. *Macromolecules* **43**(16): 6716−6723 (2010)

[21] Zhu Y G, Cao G S, Sun C Y, Xie J, Liu S Y, Zhu T J, Zhao X B, Yang H Y. Design and synthesis of NiO nanoflakes/graphene nanocomposite as high performance electrodes of pseudocapacitor. *RSC Advances* **3**:19409−19415 (2013)

[22] Ren G N, Zhang Z Z, Zhu X T, Ge B, Guo F, Men X H, Liu W M. Influence of functional graphene as filler on the tribological behaviors of Nomex fabric/phenolic composite. *Composites: Part A* **49**: 157−164 (2013)

[23] Luo B M, Yan X B, Xu S, Xue Q J. Polyelectrolyte functionalization of graphene nanosheets as support for platinum nanoparticles and their applications to methanol oxidation. *Electrochimica Acta* **59**: 429−434 (2012)

[24] Manfredi L B, Delasa O, GalegoFerna´ndez N, Va´zquez A. Structure-properties relationship for resols with different formaldehyde/phenol molar ratio. *Polymer* **40**: 3867−3875 (1999)

[25] Wang G, Yang J, Park J, Guo X, Wang B, Liu H, Yao J. Facile synthesis and characterization of graphene nanosheets. *J Phys Chem C* **112**(22): 8192−8195 (2008)

[26] Song H J, Zhang Z Z, Men X H. The tribological behaviors of the polyurethane coating filled with nano-$SiO_2$ under different lubrication conditions. *Composites: Part A* **39**: 188−194 (2008)

[27] Stuart B H. Surface plasticisation of poly(ether ether ketone) by chloroform. *Polym Testing* **16**: 49−57 (1997)

[28] Song H J, Zhang Z Z, Men X H. Tribological behavior of polyurethane-based composite coating reinforced with $TiO_2$ nanotubes. *Eur Polym J* **43**: 4092−4102 (2007)

[29] Berman D, Erdemir A, Sumant A V. Reduced wear and friction enabled by graphene layers on sliding steel surfaces in dry nitrogen. *Carbon* **54**: 454−459 (2013)

[30] Park S J, Kim B J. Roles of acidic functional groups of carbon fiber surfaces in enhancing interfacial adhesion behavior. *Mater Sci Eng A* **408**: 269−273 (2005)

[31] Park D C, Kim S S, Kim B C, Lee S M, Lee D G. Wear characteristics of carbon-phenolic woven composites mixed with nano-particles. *Composite Structures* **74**: 89−98 (2006)

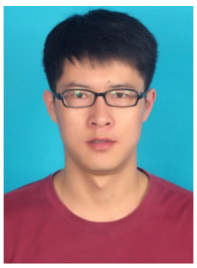

**Mingming YANG.** He is currently a PhD student at Lanzhou Institute of Chemical Physics, Chinese Academy of Sciences. He received his Bachelor degree in Chemistry from Longdong University in 2012. He joined prof. Zhaozhu Zhang's group at Lanzhou Institute of Chemical Physics in 2012. His current research interests are focused on improving the tribological properties of the polymer composite coating, fabric reinforced composite and studying the corresponding mechanism.

**Xuehu MEN.** He is currently an associate professor at Lanzhou Institute of Chemical Physics, Chinese Academy of Sciences. He received his BS degree from Lanzhou University in 2001 and a PhD degree from Lanzhou Institute of Chemical Physics in 2009. His current research interests include the development of polymer composite materials and carbon based materials for lubrication and designing materials with special surface wettability. He is the author of more than 60 journal papers and several patent applications.

**Zhaozhu ZHANG.** He is currently a group leader at Lanzhou Institute of Chemical Physics, Chinese Academy of Sciences. He received his PhD degree from Lanzhou Institute of Chemical Physics in 1998. His current research interests cover the tribology of composite materials, designing functional surfaces with special wetting behavior, and engineering coatings for drag-reduction. He has published over 150 journal papers and gained a number of national scientific awards.